Extension of Haskind's relations to cylindrical wave fields in the context of an interaction theory

Francesc Fabregas Flavià, Alain H. Clément

Extension of Haskind's relations to cylindrical wave fields in the context of an interaction theory

F. Fàbregas Flavià[a,*], A. H. Clément[a]

[a] *Ecole Centrale de Nantes, LHEEA, UMR CNRS 6598, Nantes (France)*

Abstract

The Direct Matrix Method Interaction Theory (IT) proposed by [1] speeds up the computation of hydrodynamic coefficients for large arrays of bodies when compared to direct calculations using standard Boundary Element Method (BEM) solvers. One of the most computationally expensive parts of the matrix method is the calculation of two hydrodynamic operators, known as Diffraction Transfer Matrix (DTM) and Radiation Characteristics (RC), which describe the way an isolated geometry scatters and radiates waves, respectively. A third operator, called Force Transfer Matrix (FTM), was introduced by [2] to facilitate the calculation of the forces exerted on the bodies. In this paper, a novel set of relations between the FTM and RC components is obtained using the Kochin functions specific to the cylindrical basis solutions. They extend the classical Haskind's relations, valid with incident plane waves, to the cylindrical components of the scattered and radiated fields. Moreover, an alternative demonstration of the identities is given, which does not rely on the far-field asymptotic representation of the potential. Additional expressions are provided that relate the hydrodynamic coefficients and the RC for isolated bodies as well as for arrays, and numerical checking of the derived mathematical expressions is presented. These new relations can be used to speed up calculation of the hydrodynamic operators required for the use of the IT and to test its accuracy.

Keywords: Interaction Theory, Force Transfer Matrix, Radiation

*Corresponding author

Email address: francesc.fabregas-flavia@ec-nantes.fr (F. Fàbregas Flavià)

1. Introduction

The finite-depth Direct Matrix Method interaction theory (IT) proposed by [1] enables efficient solution of the multiple-scattering problem [3] for large arrays of identical floating bodies. It requires two hydrodynamic operators, known as Diffraction Transfer Matrix (DTM) and Radiation Characteristics (RC), which model the way a body scatters and radiates waves respectively. A method for calculating these operators was presented by [1] and generalization to bodies of arbitrary shape is attributed to [4].

The IT has been used in various contexts, such as hydrodynamic interactions between vessels [5, 6], large fields of ice floes in the marginal ice zone [7] and very large floating structures [8]. [2] applied it to large arrays of wave energy converters and derived a novel method for computing both the DTM and a new operator referred to as Force Transfer Matrix (FTM). Recently, [9] illustrated the frequency-dependent patterns of the DTM and the RC, and compared the methodologies of [2] and [4].

Expression of the excitation forces of an isolated body in terms of the radiation Kochin function is a classical result of hydrodynamics [10, 11] and can be obtained by substituting the far-field representation of the radiation potential in the Haskind's relation [12]. Following a different procedure, the radiation damping coefficients for an isolated body can also be related to the radiation Kochin function. Both identities have been generalized to arrays of bodies [10, 11]. As shown by [13], the Kochin function is closely linked to the asymptotic form at infinity of the cylindrical solution to the multiple-scattering boundary value problem obtained from the IT.

In section 2, we introduce this Kochin function representation into the relations between the radiation Kochin function and both the excitation forces and the radiation damping coefficients for isolated bodies. As a result, simple relationships are obtained between the RC and the FTM on the one hand, and

between the radiation damping coefficients and the FTM on the other. To the authors' knowledge, these identities have not previously been presented in this form in the literature. An alternative derivation of the RC-FTM relation that does not require use of its far-field representation is also demonstrated, using Haskind's relation and the properties of Hankel functions. A derivation of the relationship between the radiation damping coefficients and the RC that makes use of the asymptotic properties of Bessel functions of the first and second kind is provided for completeness.

In section 3, the relationships between the RC and the excitation forces and between the radiation damping coefficients and the RC are generalized to arrays of bodies. In this case, incorporation of the complex scattered coefficients solution of the multiple-scattering problem is required.

Finally, the obtained identities are verified numerically, both for an isolated truncated vertical cylinder, and for an array of four cylinders. For the latter case, results are compared with validation data generated by [14] for an arrangement of the bodies prone to the phenomena of near-trapped modes; good agreement is obtained.

2. Isolated body

The first step of the method (hereafter referred to as IT) proposed by [1], for solving the multiple-scattering problem for an array of identical bodies is to characterize the way an isolated geometry scatters and radiates waves. Both wave fields, as well as the ambient incident plane waves, can be represented as a cylindrical eigenfunction expansion. When embedded into the classical form of Haskind's Relation [12], novel expressions relating the terms of the hydrodynamic operators required by the IT are obtained.

2.1. Haskind's Relation

Haskind's Relation [12] enables the excitation force to be expressed in terms of radiation parameters. In this section we provide a brief reminder of its derivation, which can be found for instance in [15].

The excitation force acting on a body with wetted surface S_b (Figure 1) can be written as:

$$F_{ex}^k = i\omega\rho \int_{S_b} (\phi^I + \phi^S) n^k dS \tag{1}$$

where ϕ^I is the incident potential, ϕ^S the scattered potential, n^k the generalized direction cosine with respect to S_b and ω the angular frequency.

The boundary condition on the radiation potential $\phi^{R,k}$, corresponding to degree of freedom k, is:

$$n^k = \frac{\partial \phi^{R,k}}{\partial n} \tag{2}$$

where $\phi^{R,k}$ is the radiated potential in the k-th degree of freedom.

In addition, the radiation boundary condition at infinity on $\phi^{R,k}$ reads:

$$\frac{\partial \phi^{R,k}}{\partial r} = ik_0\phi^{R,k} + O(k_0 r)^{-3/2} \quad k_0 r \to \infty \tag{3}$$

As both the scattered (ϕ^S) and the radiated (ϕ^R) potentials satisfy both the free surface boundary condition and the radiation condition at infinity, it follows from Green's theorem that:

$$\int_{S_b} \left(\phi^S \frac{\partial \phi^{R,k}}{\partial n} - \frac{\partial \phi^S}{\partial n} \phi^{R,k} \right) dS = 0 \tag{4}$$

By substituting (2) into (1) and by making use of (4), we have:

$$F_{ex}^k = i\omega\rho \int_{S_b} \left(\phi^I \frac{\partial \phi^{R,k}}{\partial n} + \phi^{R,k} \frac{\partial \phi^S}{\partial n} \right) dS \tag{5}$$

Finally, expression (5) can be rewritten by making use of the diffraction boundary condition on the wetted surface of the body:

$$\frac{\partial \phi^S}{\partial n} = -\frac{\partial \phi^I}{\partial n} \tag{6}$$

leading to the Haskind relation:

$$F_{ex}^k = i\omega\rho \int_{S_b} \left(\phi^I \frac{\partial \phi^{R,k}}{\partial n} - \phi^{R,k} \frac{\partial \phi^I}{\partial n} \right) dS \tag{7}$$

even more simply:

$$F_{ex}^k = i\omega\rho \int_{S_b} \left(\phi^I n^k - \phi^{R,k} \frac{\partial \phi^I}{\partial n} \right) dS \tag{8}$$

- a powerful formula that allows evaluation of the excitation force without solving the diffraction problem explicitly.

2.2. Eigenfunction expansion of the scattered potentials

The radiated wave field of an isolated geometry in the context of the IT in [1] is expressed using a basis of cylindrical eigenfunctions defined with respect to a local cylindrical coordinate system. These are generally referred to as outgoing partial cylindrical waves, and are combined to form a series expansion composed of both progressive waves propagating to the far-field, and evanescent standing waves responsible for adapting of the local flow to the body boundary condition in the near-field. In this form, the radiation potential reads:

$$\phi^{R,k}(r,\theta,z) = \phi_F^{R,k}(r,\theta,z) + \phi_N^{R,k}(r,\theta,z) = f(z)\Lambda^{R,k}(r,\,\theta) + \Gamma^{R,k}(r,\,\theta,\,z) \quad (9)$$

with:

$$f(z) = \frac{\cosh\, k_0(z+d)}{\cosh\, k_0 d} \quad (10)$$

$$\Lambda^{R,k}(r,\,\theta) = \sum_{m=-\infty}^{\infty} R_{0m}^k\, H_m(k_0 r)\, e^{im\theta} \quad (11)$$

$$\Gamma^{R,k}(r,\,\theta,\,z) = \sum_{m=-\infty}^{\infty}\sum_{n=1}^{\infty} \sigma_n(z)\, R_{nm}^k\, K_m(k_n r)\, e^{im\theta} \quad (12)$$

$$\sigma_n(z) = \cos\, k_n(z+d) \quad (13)$$

where $\phi_F^{R,k}$ and $\phi_N^{R,k}$ are the far-field and near-field contributions of $\phi^{R,k}$ respectively, H_m is the m-th order Hankel function of the first kind, K_m is the m-th order modified Bessel function of the second kind, d the water depth, R_{nm}^k are complex radiated cylindrical wave coefficients which shall be referred to herein as Radiation Characteristics (RC), and k_0 and k_n are the wave numbers obtained from the following dispersion equations:

$$k_0 \tanh(k_0 d) = \frac{\omega^2}{g}; \quad k_n \tan\, k_n d = -\frac{\omega^2}{g} \quad (14)$$

2.3. Eigenfunction expansion of incoming potentials

Implementation of the interaction theory involves expressing the potentials of all waves incident on the body on a basis of cylindrical eigenfunctions. These include the incident plane wave on a single body, but also, when it is part of

an array, the potential of all waves scattered by other bodies and incident on the current body. All these wave systems can be expressed as a superposition of incident partial cylindrical waves by making use of a fundamental property of Bessel functions [16]. This leads to the following expression for any incident wave potential:

$$\phi^I(r,\theta,z) = \phi_F^I(r,\theta,z) + \phi_N^I(r,\theta,z) = f(z)\Lambda^I(r,\,\theta) + \Gamma^I(r,\,\theta,\,z) \tag{15}$$

with:

$$f(z) = \frac{\cosh\, k_0(z+d)}{\cosh\, k_0 d} \tag{16}$$

$$\Lambda^I(r,\,\theta) = \sum_{m=-\infty}^{\infty} a_{0m}^I\, J_m(k_0 r)\, e^{im\theta} \tag{17}$$

$$\Gamma^I(r,\,\theta,\,z) = \sum_{m=-\infty}^{\infty}\sum_{n=1}^{\infty} \sigma_n(z)\, a_{nm}^I\, I_m(k_n r)\, e^{im\theta} \tag{18}$$

$$\sigma_n(z) = \cos\, k_n(z+d) \tag{19}$$

where ϕ^I is the total incident potential, with ϕ_F^I and ϕ_N^I its far-field and near-field contributions respectively, J_m is the m-th order Bessel function of the first kind, I_m the m-th order modified Bessel function of the first kind, and a_{0m}^I and a_{nm}^I are complex ambient incident cylindrical wave coefficients, which are functions only of the wave frequency ω and its propagation direction β.

As a particular case among these incident wave field components, the ambient incident wave is composed of only progressive terms, and can therefore be expressed without any near-field contribution ($\Gamma^I = 0$). In the context of the multiple-scattering method, however, in which scattered and radiated waves generated by a body become incident to the neighbouring ones, it becomes important to account for the near-field as well, especially when the bodies stand in close proximity to each other.

2.4. Relationship between the Force Transfer Matrix and the Radiation Characteristics

The Haskind relation (7) in 2.1 is used as a starting point for the following derivation. To begin with, the excitation force (F_{ex}^k) is expressed using the

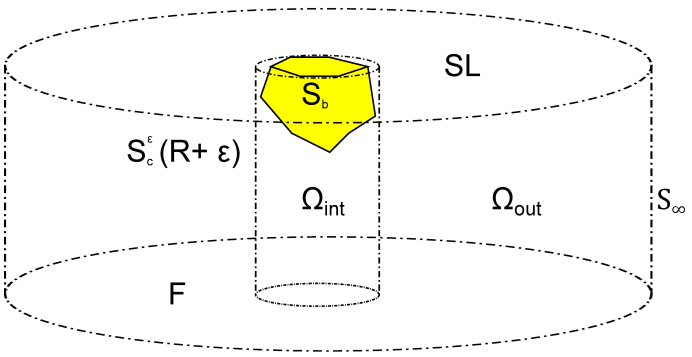

Figure 1: Schematic of the domains used for the application of the Green's theorem. Free surface (SL); body's wetted surface (S_b); body's circumscribing cylinder radius (R_c); cylindrical surface infinitesimally larger than the body's circumscribing cylinder (S_c^ϵ), seabed (F); limit of the domain at infinity (S_∞); domain interior to the circumscribing cylinder (Ω_{int}); domain comprised between the circumscribing cylinder and the cylindrical surface at infinity (Ω_{out}).

definition of the FTM ($\mathbf{G}$) given by [2] as:

$$F_{ex}^k = \sum_{m=-\infty}^{\infty} \mathbf{G}_{0m}^k a_{0m}^I \tag{20}$$

where $\mathbf{G}_{0m}^k$ corresponds to the m-th element of the k-th row of the FTM and a_{0m}^I represents the m-th term of the ambient incident wave cylindrical coefficients vector.

Direct substitution of (20) into (7) leads to:

$$\sum_{m=-\infty}^{\infty} \mathbf{G}_{0m}^k a_{0m}^I = i\omega\rho \int_{S_b} \left(\phi^I \frac{\partial \phi^{R,k}}{\partial n} - \phi^{R,k} \frac{\partial \phi^I}{\partial n} \right) dS \tag{21}$$

The expressions of the incident and radiated potentials using the base of partial cylindrical wave functions are only valid outside the circumscribing cylinder of the body (Ω_{out}) (Figure 1). Thus, by means of Green's theorem, we seek to express the surface integral in expression (21) on a control surface instead of on the body's wetted surface (S_b). Generally, a cylinder of infinite radius is used together with the asymptotic expression of the potential. In this case, we have chosen a cylindrical surface infinitesimally larger than the body's circumscribing cylinder (S_c^ϵ) to allow for the use of Green's theorem in the fluid domain (Ω_{int})

limited by S_b, S_c^ϵ, the free-surface and the seabed (Figure 1):

$$\int_{S_c^\epsilon + S_b} \left(\phi^I \frac{\partial \phi^{R,k}}{\partial n} - \phi^{R,k} \frac{\partial \phi^I}{\partial n} \right) dS = 0 \tag{22}$$

in which it is implicit that the contribution from the integrals on the free surface and the seabed are zero.

By using (22), expression (21) can be written as:

$$\sum_{m=-\infty}^{\infty} \mathbf{G}_{0m}^k a_{0m}^I = -i\rho\omega \int_{S_c^\epsilon} \left(\phi^I \frac{\partial \phi^{R,k}}{\partial n} - \phi^{R,k} \frac{\partial \phi^I}{\partial n} \right) dS \tag{23}$$

Now, substituting the expressions of the radiated (9) and incident (15) potentials into (23), and taking $\Gamma^I = 0$ for the ambient incident wave, we have:

$$\sum_{m=-\infty}^{\infty} \mathbf{G}_{0m}^k a_{0m}^I = -i\rho\omega \int_{-d}^{0} f(z)^2 dz \int_0^{2\pi} \left(\Lambda^I \frac{\partial \Lambda^{R,k}}{\partial n} - \Lambda^{R,k} \frac{\partial \Lambda^I}{\partial n} \right) R^\epsilon \, d\theta - i\rho\omega \int_{-d}^{0} \int_0^{2\pi} \left(f(z)\Lambda^I \frac{\partial \Gamma^{R,k}}{\partial n} - \Gamma^{R,k} f(z) \frac{\partial \Lambda^I}{\partial n} \right) R^\epsilon \, d\theta dz \tag{24}$$

where R^ϵ is the radius of a cylindrical surface infinitesimally larger than the body's circumscribing cylinder.

With respect to the first term on the right hand side of (24), the depth integral is evaluated using:

$$\omega \int_{-d}^{0} f(z)^2 dz = \frac{c_g}{k_0} \frac{\omega^2}{g} \tag{25}$$

where c_g is the group velocity given by:

$$c_g = \frac{1}{2} \frac{\omega}{k_0} \left(1 + \frac{2k_0 d}{\sinh 2k_0 d} \right) \tag{26}$$

For convenience we define the first integral in θ to be I:

$$I = \int_0^{2\pi} \left(\Lambda^I \frac{\partial \Lambda^{R,k}}{\partial n} - \Lambda^{R,k} \frac{\partial \Lambda^I}{\partial n} \right) R^\epsilon \, d\theta \tag{27}$$

Substituting the definitions of Λ^I and $\Lambda^{R,k}$ into the previous expression:

$$I = \int_0^{2\pi} \left(\sum_{m=-\infty}^{\infty} a_{0m}^I J_m(k_0 r) \sum_{q=-\infty}^{\infty} R_{0q}^k \frac{\partial H_q(k_0 r)}{\partial n} \, |_{r=R^\epsilon} \right) e^{i(m+q)\theta} R^\epsilon d\theta - \int_0^{2\pi} \left(\sum_{m=-\infty}^{\infty} a_{0m}^I \frac{\partial J_m(k_0 r)}{\partial n} \, |_{r=R^\epsilon} \sum_{q=-\infty}^{\infty} R_{0q}^k H_q(k_0 r) \right) e^{i(m+q)\theta} R^\epsilon d\theta \tag{28}$$

The only non-zero contributions of the terms $e^{i(m+q)\theta}$ to the integral in θ come from the case where $m = -q$ and they are equal to 2π. Thus, (28) can be rewritten:

$$I = 2\pi R^{\epsilon} \sum_{m=-\infty}^{\infty} a_{0m}^{I} R_{0-m}^{k} \left(J_m(k_0 r) \frac{\partial H_{-m}(k_0 r)}{\partial r} - \frac{\partial J_m(k_0 r)}{\partial r} H_{-m}(k_0 r) \right) \tag{29}$$

The expression in parentheses in (29) can be rewritten using the following identities for Bessel and Hankel functions [17]:

$$J_m = \frac{1}{2}(H_m^{(1)} + H_m^{(2)}) \tag{30}$$

$$H_{-m}^{(1)} = (-1)^m H_m^{(1)} \tag{31}$$

leading to:

$$I = 2\pi R^{\epsilon} \sum_{m=-\infty}^{\infty} a_{0m}^{I} R_{0-m}^{k} \frac{1}{2}(-1)^m \left(H_m^{(2)}(k_0 r) \frac{\partial H_m^{(1)}(k_0 r)}{\partial r} \mid_{r=R^{\epsilon}} - \frac{\partial H_m^{(2)}(k_0 r)}{\partial r} \mid_{r=R^{\epsilon}} H_m^{(1)}(k_0 r) \right) \tag{32}$$

The term in brackets can now be related to the Wronskian of $H_m^{(1)}$ and $H_m^{(2)}$ [17]:

$$- W(H_m^{(1)}, H_m^{(2)}) = H_m^{(2)}(k_0 r) \frac{\partial H_m^{(1)}(k_0 r)}{\partial r} \mid_{r=R^{\epsilon}} - \frac{\partial H_m^{(2)}(k_0 r)}{\partial r} \mid_{r=R^{\epsilon}} H_m^{(1)}(k_0 r) = -\frac{4i}{\pi R^{\epsilon}} \tag{33}$$

Substituting (33) into (32):

$$I = 4i \sum_{m=-\infty}^{\infty} (-1)^m a_{0m}^{I} R_{0-m}^{k} \tag{34}$$

Let us now evaluate the second term of the summation on the right hand side of equation (24). We define the first and second terms of the integral in θz to be:

$$I_2 = \int_{-d}^{0} \int_{0}^{2\pi} f(z) \Lambda^I \frac{\partial \Gamma^{R,k}}{\partial r} R^{\epsilon} d\theta dz \tag{35}$$

$$I_3 = \int_{-d}^{0} \int_{0}^{2\pi} f(z) \Gamma^{R,k} \frac{\partial \Lambda^I}{\partial r} R^{\epsilon} d\theta dz \tag{36}$$

Considering I_2 first, we substitute the definitions of Λ^I and $\Gamma^{R,k}$ given by (17) and (12) respectively to obtain:

$$I_2 = \int_{-d}^{0}\int_{0}^{2\pi} \Big(\sum_{m=-\infty}^{\infty} f(z) a^I_{0m}\, J_m(k_0 r) \mid_{r=R^\epsilon} \times \sum_{q=-\infty}^{\infty}\sum_{n=1}^{\infty} \sigma_n(z) R^k_{nq} \frac{\partial K_q(k_n r)}{\partial r} \mid_{r=R^\epsilon} \Big) e^{i(m+q)\theta}\, R^\epsilon d\theta dz \quad (37)$$

The only non-zero contributions of the terms $e^{i(m+q)\theta}$ to the integral in θ arise where $m = -q$ and they are equal to 2π. Thus, (37) reads:

$$I_2 = 2\pi R^\epsilon \sum_{m=-\infty}^{\infty}\sum_{n=1}^{\infty} a^I_{0m}\, R^k_{n,-m} \times J_m(k_0 r) \frac{\partial K_{-m}(k_n r)}{\partial r} \mid_{r=R^\epsilon} \int_{-d}^{0} f(z)\sigma_n(z) dz \quad (38)$$

By means of the orthogonality properties of the depth functions:

$$\int_{-d}^{0} \cosh\, k_0(d+z) \cos\, k_n(d+z) dz = 0 \quad (39)$$

the depth integral in (38) vanishes. An analogous reasoning can be applied to I_3, and so finally:

$$I_2 = I_3 = 0 \quad (40)$$

This shows that the second term of the summation on the right hand side of equation (24), i.e. the near-field contribution of the radiated potential, has no effect on the excitation force. Finally, (23) becomes:

$$\sum_{m=-\infty}^{\infty} \mathbf{G}^k_{0m} a^I_{0m} = 4\frac{\rho c_g \omega^2}{g k_0} \sum_{m=-\infty}^{\infty} (-1)^m R^k_{0-m} a^I_{0m} \quad (41)$$

This relation between the FTM and the RC expresses the original Haskind relation in the framework of cylindrical wave fields theory. Furthermore, as each partial wave is an eigenfunction of an orthogonal set, the identity (41) holds element-wise and reads:

$$\mathbf{G}^k_m = 4\frac{\rho c_g \omega^2}{g k_0} (-1)^m R^k_{-m} \quad (42)$$

In (42), the subindex n referring to evanescent terms has been omitted to simplify notation. Hereafter, a single subindex will indicate that only the far-field contribution to the potential is considered.

In the above derivation, the integration surface was chosen to be the circumscribing cylinder to the body. However, it was observed that the radius of the cylindrical control surface cancels out when the integral is evaluated. Thus, it would have been equivalent to consider a cylinder at infinity and retain only the leading terms of the asymptotic expression of the potential.

The expression of the excitation force in terms of the far-field radiation potential is a classical result of hydrodynamics, which can be found for instance in [10] or [18]:

$$F_{ex}^{k} = -\frac{4}{k_0}\rho g A \mathcal{A}^{k}(\theta_I + \pi) c_g \tag{43}$$

where F_{ex}^{k} is the excitation force and $\mathcal{A}^{k}(\theta)$, generally known as the Kochin function, corresponds to the angular variation of the radially spreading wave in the far-field representation of the potential. At leading order of the asymptotic expansion for large r, the potential may be expressed as:

$$\phi \sim -\frac{ig}{\omega}\frac{\cosh k_0(z+h)}{\cosh k_0 h}\mathcal{A}(\theta)\left(\frac{2}{\pi k_0 r}\right)^{\frac{1}{2}} e^{ik_0 r - i\pi/4} \tag{44}$$

Expression (43) could also have been used to obtain (41), taking into account that the Kochin function is directly related to the asymptotic form of the cylindrical solution:

$$\mathcal{A}^{k}(\theta) = \sum_{m=-\infty}^{\infty} (-i)^m \frac{i\omega}{g} R_m^k e^{im\theta} \tag{45}$$

Equation (45) has been adapted to the notation and the far-field potential representation of [10], and differs slightly from that given by [13]. Substituting (45) into (43) returns the same expression as in (41).

2.5. Radiation Damping Coefficients in terms of the far-field radiation potential

By applying Green's theorem to two radiation potentials, the radiation damping coefficients may be expressed in terms of the far-field radiation potential. This is a classic result of hydrodynamics, whose derivation is briefly reviewed in this section and can be found for instance in [18].

We consider the two radiation potentials $\phi^{R,p}$ and $(\phi^{R,k})^*$. By application of Green's theorem in the domain $\Omega_{int}\,\mathrm{U}\,\Omega_{out}$:

$$\int_{S_b}\left(\phi^{R,p}n_k-(\phi^{R,k})^*n_p\right)dS=-\int_{S_\infty}\left(\phi^{R,p}\frac{\partial(\phi^{R,k})^*}{\partial n}-(\phi^{R,k})^*\frac{\partial\phi^{R,p}}{\partial n}\right)dS \tag{46}$$

where the super-index * represents the complex conjugate.

If we apply Green's theorem again to the same domain and to the same radiation potentials (now without taking the complex conjugate of $\phi^{R,k}$) we can deduce that:

$$\int_{S_b}\phi^{R,p}\,n_k dS=\int_{S_b}\phi^{R,k}\,n_p dS \tag{47}$$

Thus:

$$\int_{S_b}(\phi^{R,p})^*\,n_k dS=\int_{S_b}(\phi^{R,k})^*\,n_p dS \tag{48}$$

By substituting (48) into (46) we obtain:

$$\mathbf{D}^{pk}=-\frac{\rho\omega}{2i}\int_{S_\infty}\left(\phi^{R,p}\frac{\partial(\phi^{R,k})^*}{\partial n}-(\phi^{R,k})^*\frac{\partial\phi^{R,p}}{\partial n}\right)dS \tag{49}$$

where $\mathbf{D}^{pk}$ represents the element p,k in the radiation damping coefficient matrix, with p the direction of the force and k the degree of freedom.

Expression (49) can be simplified using (3):

$$\mathbf{D}^{pk}=\rho\omega k_0\int_{S_\infty}\phi^{R,p}\left(\phi^{R,k}\right)^*dS \tag{50}$$

from which the symmetry of $\mathbf{D}^{pk}$ and the positivity of $\mathbf{D}^{pp}$ are easily deduced.

2.6. Relationship between the Force Transfer Matrix and the Damping coefficients

Now (50) can be used to derive a relationship between the diagonal terms of the radiation damping coefficients matrix and the FTM.

By using the definition of the far-field radiated potential in cylindrical coordinates (first term of the summation in (9)), equation (50) can be expressed

as:

$$\mathbf{D}^{pk} = \rho\omega k_0 \int_{-d}^{0} f(z)^2 dz \times$$
$$\int_0^{2\pi} \left(\sum_{m=-\infty}^{\infty} R_m^p H_m^{(1)}(k_0 r) \mid_{r=R^\infty} \sum_{q=-\infty}^{\infty} \left(R_q^k\right)^* H_q^{(2)}(k_0 r) \mid_{r=R^\infty} \right) e^{i(m-q)\theta} R^\infty d\theta \tag{51}$$

where R^∞ represents the radius of a cylindrical control surface at infinity.

The only non-zero contributions of the terms $e^{i(m-q)\theta}$ to the integral in θ occur where $m = q$ and they are equal to 2π. Thus, the previous expression can be written as:

$$\mathbf{D}^{pk} = 2\pi R^\infty \rho c_g \frac{\omega^2}{g} \sum_{m=-\infty}^{\infty} R_m^p \left(R_m^k\right)^* H_m^{(1)}(k_0 r) \mid_{r=R^\infty} H_m^{(2)}(k_0 r) \mid_{r=R^\infty} \tag{52}$$

where the depth integral has been evaluated using (25).

The product of Hankel functions of the first and the second kind can be rewritten using their definition in terms of the Bessel functions of the first and the second kind:

$$H_m^{(1)} H_m^{(2)} = (J_m + iY_m)(J_m - iY_m) = J_m^2 + Y_m^2 \tag{53}$$

where the argument of the functions has been omitted for simplicity.

The asymptotic forms ($z \to \infty$) of the Bessel functions of the first and second kind are [17]:

$$J_m(z) = \sqrt{\frac{2}{\pi z}} \cos(z - \frac{1}{2} m\pi - \frac{1}{4}\pi) + \mathbf{O}(|z|^{-1}) \tag{54}$$

$$Y_m(z) = \sqrt{\frac{2}{\pi z}} \sin(z - \frac{1}{2} m\pi - \frac{1}{4}\pi) + \mathbf{O}(|z|^{-1}) \tag{55}$$

Thus:

$$J_m^2(z) + Y_m^2(z) = \left(\sqrt{\frac{2}{\pi z}}\right)^2 (\cos^2(z - \frac{1}{2} m\pi - \frac{1}{4}\pi) + \sin^2(z - \frac{1}{2} m\pi - \frac{1}{4}\pi)) = \frac{2}{\pi z} \tag{56}$$

where the higher order terms of the asymptotic form have been neglected.

By using (56), expression (52) becomes:

$$\mathbf{D}^{pk} = 4\rho c_g \frac{\omega^2}{k_0 g} \sum_{m=-\infty}^{\infty} R_m^p \left(R_m^k\right)^* \tag{57}$$

For the diagonal terms of the damping matrix, i.e. $p = k$, using the fact that the product of a complex number and its conjugate is $z\bar{z} = |z|^2$ we have:

$$\mathbf{D}^{kk} = 4\rho c_g \frac{\omega^2}{k_0 g} \sum_{m=-\infty}^{\infty} |R_m^k|^2 \tag{58}$$

where we note that the term $4\rho c_g \frac{\omega^2}{k_0 g}$ is exactly the same as in (42).

An equivalent form for expression (57) can be derived from equation 8.6.13 in [10], which relates the damping coefficients to the Kochin function:

$$\mathbf{D}^{pk} = \frac{2}{\pi k_0} \rho g c_g \int_0^{2\pi} \mathcal{A}_p(\theta) \mathcal{A}_k^*(\theta) d\theta \tag{59}$$

where $\mathcal{A}(\theta)$ is as defined in (45).

The result in (58) gives a relationship between the diagonal terms of the radiation damping coefficients matrix and the RC. Commonly this relationship is expressed in terms of the excitation forces as [19, eq.173,p.304]:

$$\mathbf{D}^{kk} = \frac{k}{8\pi \rho g c_g} \int_0^{2\pi} |F_{ex}^k(\theta)|^2 d\theta \tag{60}$$

where $F_{ex}^k(\theta)$ is the excitation force on the fixed body due to an incident wave propagating at an angle $\pi + \theta$ to the positive x-axis.

A similar expression can be obtained by using (42), which relates the elements of the FTM and the RC, and substituting it into (58), leading to:

$$\mathbf{D}^{kk} = \frac{g k_0}{4\rho c_g \omega^2} \sum_{m=-\infty}^{\infty} |\mathbf{G}_m^k|^2 \tag{61}$$

3. Array

3.1. Generalisation of Haskind's relation for an array of bodies

Expression (7) can be generalized to an array composed of N_b bodies by following a similar derivation to that shown in section 2.1 (see for instance

[11]). In this case, the body boundary condition (2) is expressed as:

$$\frac{\partial \Phi_i^{R,k_i}}{\partial n} = \begin{cases} n^{k_i} & \text{on} \quad S_i \\ 0 & \text{on} \quad S_j \, (j \neq i) \end{cases} \tag{62}$$

where Φ_i^{R,k_i} is the potential of a wave radiated by body i in a mode of motion k_i and scattered by all the neighbouring bodies j at rest, and n^{k_i} the boundary condition on the radiation potential Φ_i^{R,k_i}.

Then, the excitation force acting on a body i of an array composed of N_b bodies can be written in terms of only the ambient and radiation potentials:

$$F_{ex,i}^{k_i} = i\rho\omega \int_S \left(\phi^I \frac{\partial \Phi_i^{R,k_i}}{\partial n} - \Phi_i^{R,k_i} \frac{\partial \phi^I}{\partial n} \right) dS \tag{63}$$

where ϕ^I represents the ambient incident potential and $S = \bigcup S_i$

By applying Green's theorem to a domain limited by surface S and a control surface at infinity (S_∞), the excitation force can be evaluated using only the far field potentials as:

$$F_{ex,i}^{k_i} = -i\rho\omega \int_{S_\infty} \left(\phi^I \frac{\partial \Phi_i^{R,k_i}}{\partial n} - \Phi_i^{R,k_i} \frac{\partial \phi^I}{\partial n} \right) dS \tag{64}$$

3.2. Relationship between the Excitation Force and the Radiation Characteristics

The representation of the incident and radiated potentials in expression (64), relating the excitation force with the far-field potentials, follows as in the far-field terms of (15) and (9) respectively. However, as the body is no longer in isolation, the radiated potential of a body i moving in mode of motion k_i will be written as a sum of two contributions:

$$\Phi_i^{R,k_i} = \phi_i^{R,k_i} + \sum_{j=1}^{N_b} \phi_j^{S,k_i} \tag{65}$$

where Φ_i^{R,k_i} is the total radiated potential, ϕ_i^{R,k_i} is the radiated potential by body i in motion mode k_i as if it was isolated and ϕ_j^{S,k_i} is the potential scattered

by a body j in the array due to the wave radiated by body i moving in mode of motion k_i.

Using the far-field terms of (15) and (9), together with the fact that the scattered potential can be expressed in terms of the same partial cylindrical wave functions as the radiated potential, we obtain:

$$\phi_i^{R,k_i}(r_i,\theta_i,z_i) = f(z)\sum_{m=-\infty}^{\infty} R_{im}^{k_i}\, H_m(k_0 r_i)\, e^{im\theta_i} \tag{66}$$

$$\phi_j^{S,k_i}(r_j,\theta_j,z_j) = f(z)\sum_{m=-\infty}^{\infty} A_{jm}^{S,k_i}\, H_m(k_0 r_j)\, e^{im\theta_j} \tag{67}$$

where A_j^{S,k_i} represent the complex cylindrical partial wave coefficients of the scattered potential by body j due to the motion of body i in motion mode k_i.

As the potentials are expressed with respect to the local cylindrical reference system centered at each body, we apply a coordinate transformation to express all potentials with respect to the local reference system of body i. To express the far-field coefficients from different sources with respect to a common origin, [18] uses the asymptotic approximations for the relationship between local and global coordinates. In this case, we make use of the multipole expansion matrix $\mathbf{M}_{ij}$ from Graff's addition theorem, which expresses the scattered potential of body i around the origin of the j-th coordinate system [8]:

$$\Upsilon_i^S(r_i,\theta_i,z_i) = \mathbf{M}_{ij}\,\Upsilon_j^S(r_j,\theta_j,z_j) \tag{68}$$

where $\Upsilon^S = H_m(k_0 r)\, e^{im\theta}$ and the progressive terms of the multipole expansion matrix are given by:

$$(\mathbf{M}_{ij})_{nn}^{mq} = J_{m-q}(k_0 L_{ij})\, e^{i(m-q)\alpha_{ij}};\quad n=0 \tag{69}$$

where L_{ij} is the separating distance between bodies i and j, α_{ij} the angle at body i between the positive x-direction and the line joining the center of i to that of j in an anti-clockwise direction (Figure 2), indices m, q the angular-mode, and n the depth-mode.

By applying (68) and using (66) and (67), equation (65) can be expressed

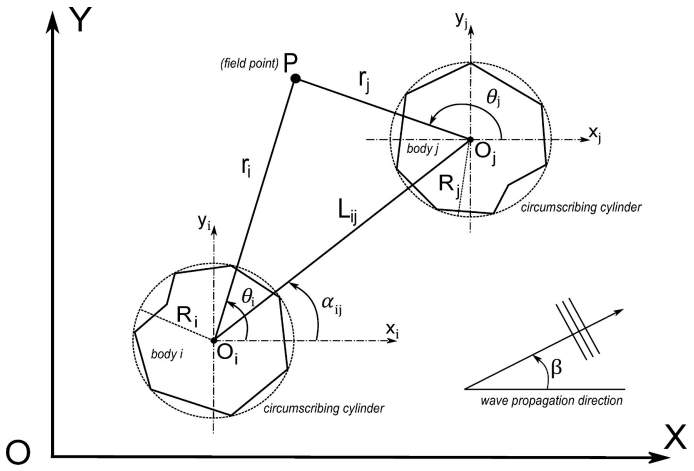

Figure 2: Schematic of the plane view of two bodies of arbitrary geometry with the nomenclature and reference systems used in this paper.

as:

$$\Phi_i^{R,k_i}(r_i,\theta_i,z_i) = f(z)\sum_{m=-\infty}^{\infty}\mathcal{R}_{im}^{k_i}H_m(k_0r_i)e^{im\theta_i} \tag{70}$$

where $\mathcal{R}_i^{k_i}$ is the vector of cylindrical coefficients expressing the radiated wave by body i in a motion mode k and including all the scattered waves by all the bodies in the array:

$$(\mathcal{R}_i^{k_i})_m = \left(R_i^{k_i} + \sum_{j=1}^{N_b}[\mathbf{M}_{ji}]^T A_j^{k_i}\right)_m \tag{71}$$

Finally, expression (64) can be evaluated in the same manner as (23), leading to:

$$F_{ex,i}^{k_i} = 4\frac{\rho c_g\omega^2}{gk_0}\sum_{m=-\infty}^{\infty}(-1)^m a_m^{I,i}\,\mathcal{R}_{i-m}^{k_i} \tag{72}$$

By separating the contributions from vector (71), the excitation force acting on body i in direction k_i can also be expressed as:

$$F_{ex,i}^{k_i} = \sum_{m=-\infty}^{\infty}\left(\mathbf{G}_m^{k_i} + \tilde{\mathbf{G}}_m^{k_i}\right)a_m^{I,i} \tag{73}$$

where $\tilde{\mathbf{G}}_m^{k_i}$ is defined as:

$$\tilde{\mathbf{G}}_m^{k_i} = 4\frac{\rho c_g \omega^2}{g k_0}(-1)^m \left(\sum_{j=1}^{N_b} [\mathbf{M}_{ji}]^T \, A_j^{k_i} \right)_m \tag{74}$$

In (73) we have separated the contributions to the excitation force from the body itself, as if it was isolated (first term of the summation), and from the hydrodynamic interactions with the rest of bodies in the array (second term).

Equation (72) could also have been derived, for instance, from expression 5.203 in [18], which is a generalization of (43) for an array of bodies and relates the excitation force on a body to the radiation far-field expressed at a global origin, by substituting in it the expression of the Kochin function defined in (45). In this case, the RC of the isolated body should be replaced by the vector of cylindrical coefficients expressing the radiated wave by a body in the array, including all the scattered waves by the neighbours, as in (71).

3.3. Relationship between the Damping coefficients and the Radiation Potential

Similarly to the result presented in section 2.5, the radiation damping of a body in the array can be expressed in terms of the far-field radiation potential. Using this generalization, the damping force on oscillator i in a direction k_i due to a unit velocity motion of body j moving in a mode of motion k_j can be expressed as [11]:

$$\mathbf{D}_{ij}^{p_i,k_j} = \rho\omega k_0 \int_{S_\infty} \Phi_j^{R,k_j} \left(\Phi_i^{R,p_i} \right)^* dS \tag{75}$$

where $\mathbf{D}_{ij}^{p_i,k_j}$ is the radiation damping force on body i in a degree of freedom p_i due to a unitary velocity of body j in a degree of freedom k_j, and Φ_j^{R,k_j} and Φ_i^{R,p_i} are respectively the radiated potentials from body j in a mode of motion k_j and body i in a mode of motion p_i and scattered by the rest of the bodies in the array.

As in section 3.2, we express both potentials in the reference system local to

body i of the array, and thus:

$$\Phi_i^{R,p_i}(r_i,\theta_i,z_i) = f(z)\sum_{m=-\infty}^{\infty}\mathcal{R}_{im}^{p_i}H_m(k_0r_i)\,e^{im\theta_i} \tag{76}$$

$$\Phi_j^{R,k_j}(r_i,\theta_i,z_i) = f(z)\sum_{m=-\infty}^{\infty}\mathcal{R}_{jm}^{k_j}H_m(k_0r_i)\,e^{im\theta_i} \tag{77}$$

where $\mathcal{R}_i^{p_i}$ and $\mathcal{R}_j^{k_j}$ are:

$$\mathcal{R}_i^{p_i} = R_i^{p_i} + \sum_{j=1}^{N_b}[\mathbf{M}_{ji}]^T\,A_j^{p_i} \tag{78}$$

$$\mathcal{R}_j^{k_j} = [\mathbf{M}_{ji}]^T R_j^{k_j} + \sum_{j=1}^{N_b}[\mathbf{M}_{ji}]^T\,A_j^{k_j} \tag{79}$$

(75) can then be evaluated in a similar manner to (50), leading to:

$$\mathbf{D}_{ij}^{p_i,k_j} = 4\frac{\rho c_g\omega^2}{gk_0}\sum_{m=-\infty}^{\infty}\mathcal{R}_{jm}^{k_j}\,(\mathcal{R}_{im}^{p_i})^* \tag{80}$$

If we set $i=j$ and $p=k$, by separating the contributions from vectors (76) and (77), expression (80) can be rewritten as:

$$\mathbf{D}_{ii}^{k_i,k_i} = \frac{gk_0}{4\rho c_g\omega^2}\sum_{m=-\infty}^{\infty}|\mathbf{G}_m^{k_i}|^2 + \frac{gk_0}{4\rho c_g\omega^2}\sum_{m=-\infty}^{\infty}\left(\mathbf{G}_{-m}^{k_i}(\tilde{\mathbf{G}}_m^{k_i})^* + (\mathbf{G}_{-m}^{k_i})^*\tilde{\mathbf{G}}_m^{k_i} + |\tilde{\mathbf{G}}_m^{k_i}|^2\right) \tag{81}$$

where the first term of the summation corresponds to the term of the damping coefficient matrix $\mathbf{D}^{k,k}$ of the body in isolation (57), and the remaining terms to the contribution from the multiple-scattering from the rest of bodies in the array.

Expression (80) can also be obtained, for instance, from equation 5.182 in [18], using the expression for the Kochin function defined in (45), in which the RC of the isolated body is replaced by the vector of cylindrical coefficients that expresses the radiated wave by a body in the array including all the scattered waves by the neighbours, as in (71).

4. Results and Discussion

In this section, the relationships derived in sections 2.4 and 2.6 are verified numerically. Results are presented for a truncated vertical circular cylinder of radius a, draft $2a$ in water depth $4a$. In addition, the excitation forces and radiation damping coefficients are computed using the identities derived in sections (3.2) and (3.3) for an array composed of four truncated vertical circular cylinders of the same geometry separated by distance $4a$ (Figure 6). This particular configuration was studied by [14] using the IT with semi-analytical expressions for the hydrodynamic operators and showed that, for certain wave numbers, it is prone to the phenomenon of near-trapped modes.

The Radiation Characteristics (RC) presented in section 2.2 enable the wave radiated by a body moving in a degree of freedom k to be expressed in the form of equation (9), and can be computed for arbitrary geometries using two different methodologies [4, 2], a comparison of which can be found in [9]. In this section the former method is used, implemented in the open-source BEM solver NEMOH [1].

The mesh used for the calculations is the same as in [9]. A sensitivity study of the angular modes truncation (M) was performed to ensure convergence of the results computed with the IT.

4.1. Isolated body

Figures 3 - 4 show the progressive terms of the FTM in surge and roll respectively, computed both by means of our BEM solver, using its capability to solve the diffraction problem for partial cylindrical waves, and by means of the RC (also computed with our BEM solver using the methodology of [4]), using the identity (42). Excellent agreement between the two approaches is observed. As mentioned in [9], only partial waves associated with angular modes $m = 1$ and $m = -1$ are required to express the radiated wave by a cylinder moving in surge. The RC are directly related to the FTM terms by expression (42), from

[1] http://lheea.ec-nantes.fr/doku.php/emo/nemoh/start

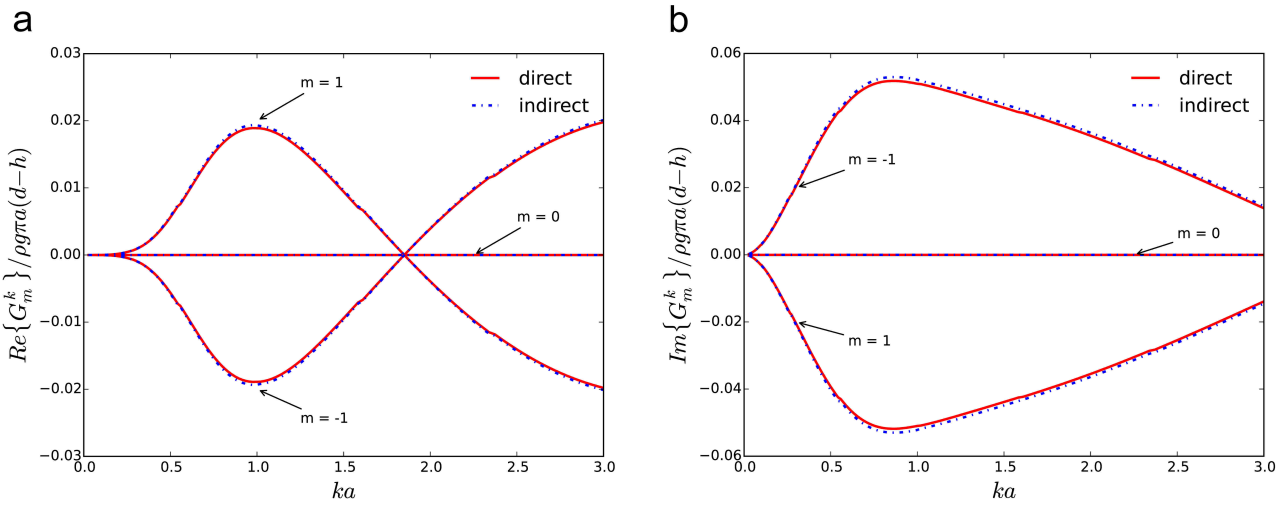

Figure 3: Real (a) and Imaginary (b) parts of the FTM progressive terms in the surge (k=1) degree of freedom for a cylinder of radius a, draft ($d-h=2a$) in a water depth ($d=4a$). The solid line (direct) corresponds to the direct calculation of the FTM using our BEM solver. The dotted line (indirect) is calculated from the RC computed with our BEM solver and by using the right-hand side of equation (42).

which it follows that only the same modes of the incident cylindrical waves will exert a force on the body.

Figure 5 shows the diagonal radiation damping coefficients for surge and roll computed in the standard manner using our BEM solver and by means of the FTM terms using the identity in (61). A very good match between results can be appreciated with a slight numerical inaccuracy of 2% for roll at the region of wavenumbers ($ka > 1.5$).

4.2. Array

Figure 7 shows the variation of the excitation force with wave number in surge and heave for cylinders 1-2 (Figure 6) and for an incident wave propagating with direction $\beta = 0$. Results obtained by [14] are shown, and compared to our computation using the IT, for which hydrodynamic operators have been obtained using our BEM solver. Very good agreement between them is found.

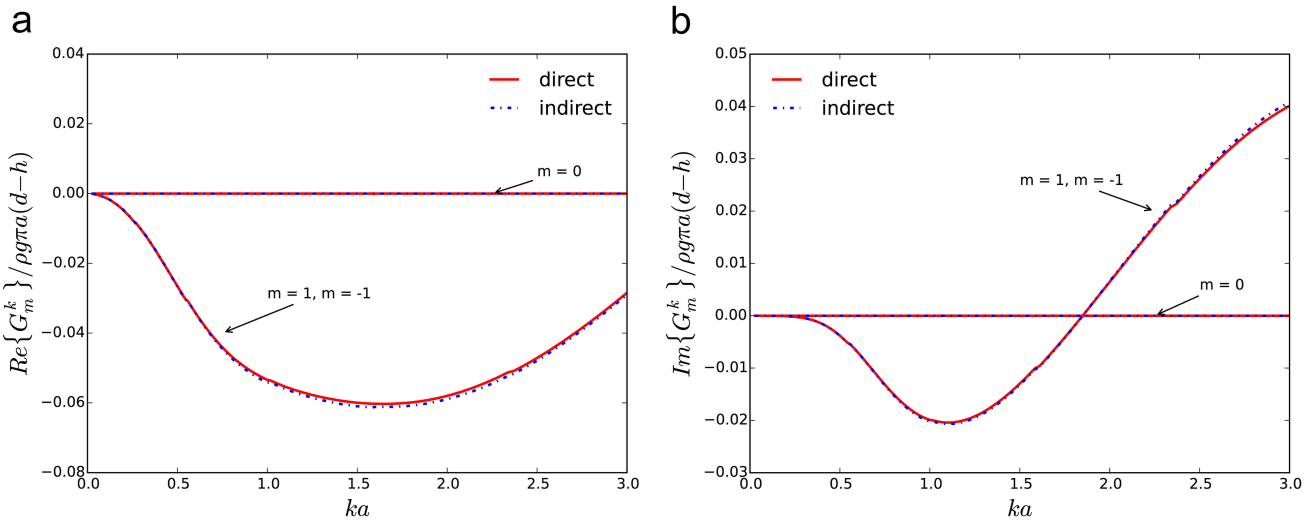

Figure 4: Real (a) and Imaginary (b) parts of the FTM progressive terms in the Roll (k=4) degree of freedom for a cylinder of radius a, draft ($d-h=2a$) in a water depth ($d=4a$). The solid line (direct) corresponds to the direct calculation of the FTM using our BEM solver. The dotted line (indirect) is calculated from the RC computed with our BEM solver and by using the right-hand side of equation (42).

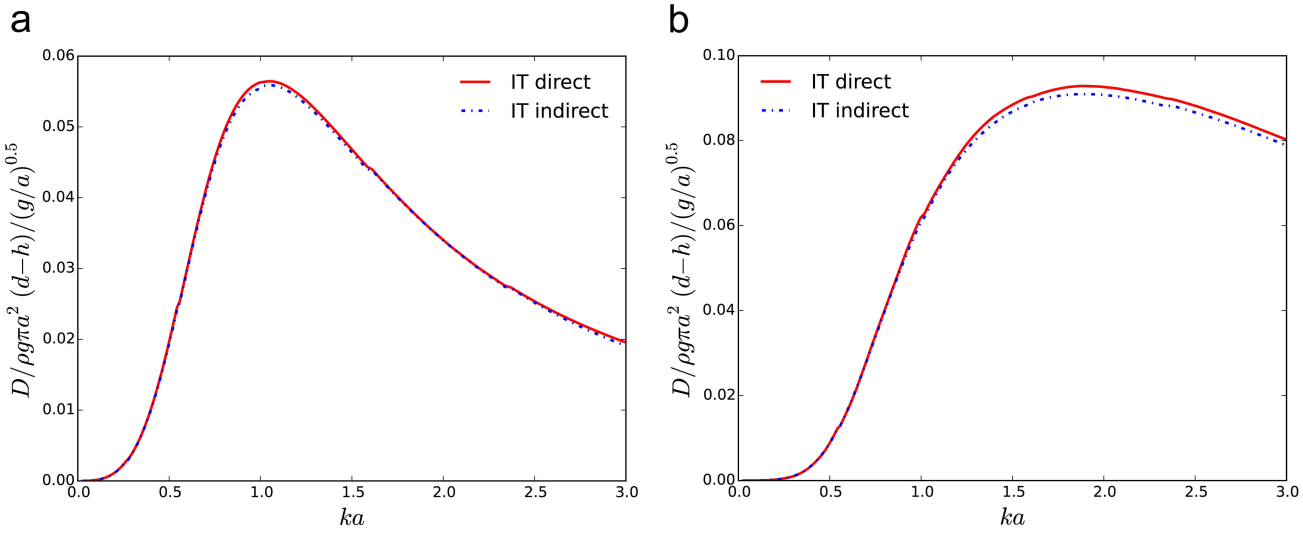

Figure 5: Diagonal radiation damping coefficients for the degrees of freedom Surge (a) and Roll (b) of a cylinder of radius a, draft ($d - h = 2a$) in a water depth ($d = 4a$). The solid line (direct) corresponds to the direct calculation of the damping coefficients using our BEM solver. The dotted line (indirect) is calculated from the FTM computed with our BEM solver and by using the right-hand side of equation (61).

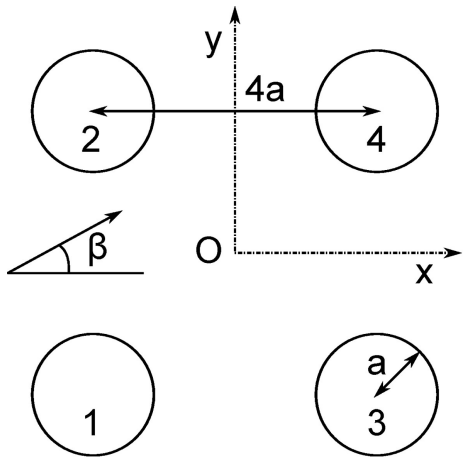

Figure 6: Schematic representation of an array composed of four truncated vertical cylinders of radius a and separated by a distance between centers $4a$. $\beta = 0$ corresponds to the positive $x - axis$.

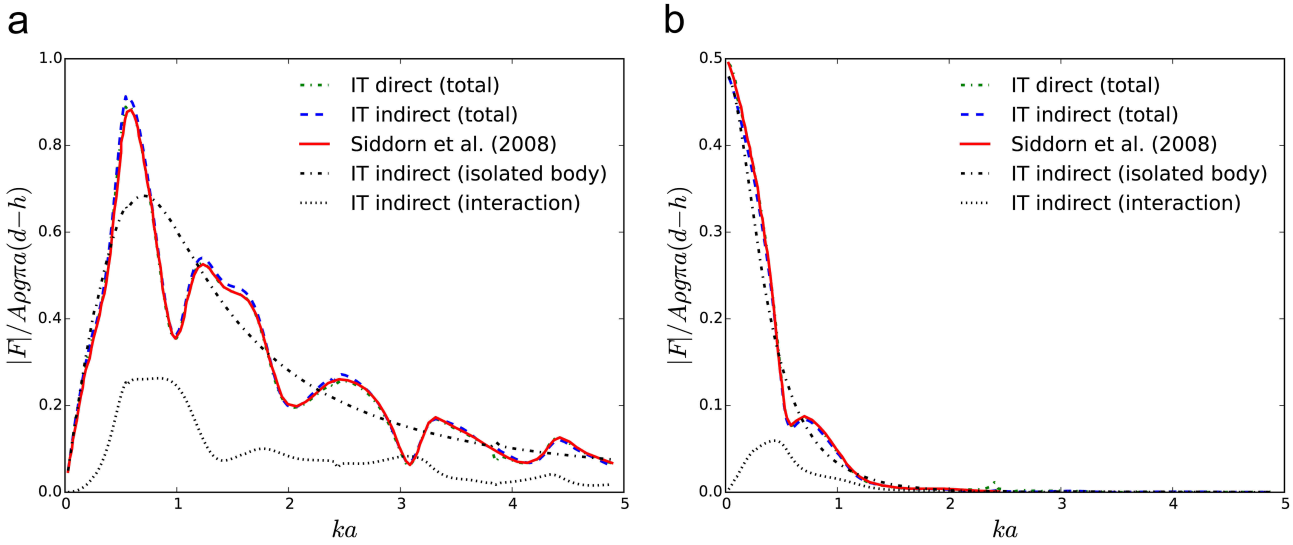

Figure 7: Non-dimensional excitation forces in Surge (a) and Heave (b) for the cylinders 1-2 in the array shown in Figure 6 from an incident plane wave with propagation direction ($\beta = 0$) and amplitude A . The solid line reproduces the results by [14]; the dotted green line has been computed with the IT by [1] by using our BEM solver to compute the required hydrodynamic operators and the dotted blue line by means of the right-hand side of equation (72). The black dotted lines $(- \cdot -\cdot)$ and $(\cdot \cdot \cdot)$ correspond respectively to the contribution to the total excitation force from the isolated body and from the hydrodynamic interactions with the neighbours and have been computed from the first and second terms of equation (73) respectively.

In addition, the excitation forces computed by means of the relationship (72) are shown. Again, very good agreement with the previous methodologies is observed, despite a slight overestimation of the peaks for surge, mainly at low wave numbers ($ka < 1$). An irregular frequency at $ka = 3.8$ (surge) and $ka = 2.4$ (heave) can also be observed. Also shown are the contributions to the total excitation force from the isolated body on one hand and from the hydrodynamic interactions on the other hand, which were computed separately using expression (73). Only the modulus is displayed here, so the curves cannot be directly summed.

One would normally compute the excitation forces using the FTM, which

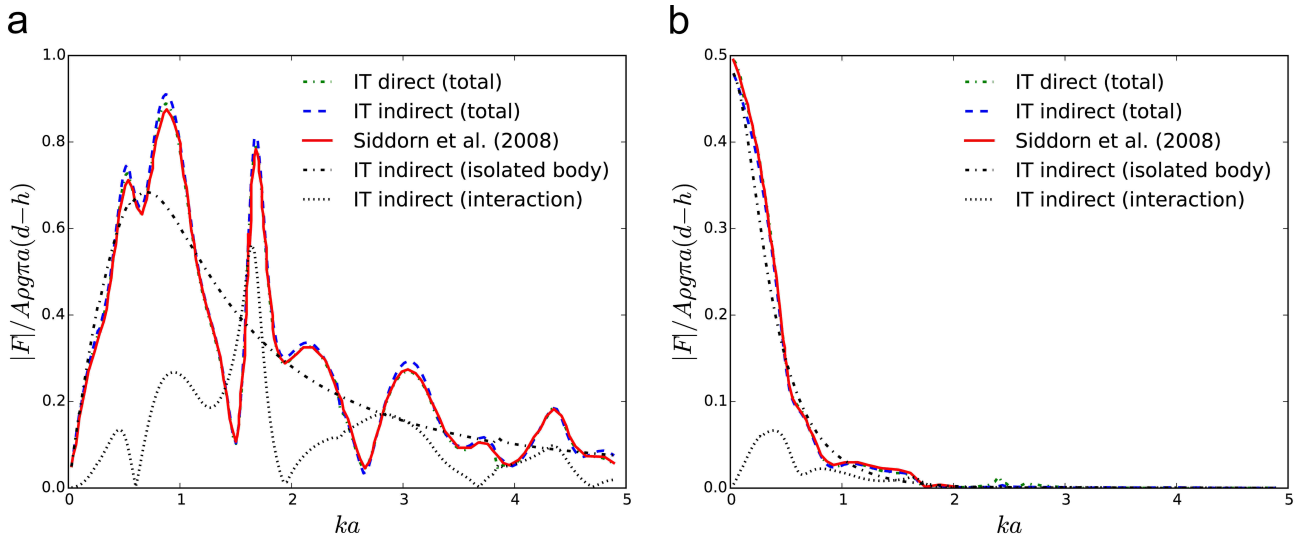

Figure 8: Non-dimensional excitation forces in Surge (a) and Heave (b) for the cylinder 1 in the array shown in Figure 6 from an incident plane wave with propagation direction ($\beta = \pi/4$) and amplitude A . The legend follows as in Figure 7

sums the individual contributions to the total excitation force from each partial incident wave by solving a diffraction problem. The verification provided by equation (72) is powerful from two points of view. First, it does not make use of diffraction, but rather the cylindrical coefficients of a radiation problem. Second, a summation of all the cylindrical coefficients is performed prior to multiplication by a scalar quantity, which can be, for instance, in the order of 10^7 times higher in magnitude than each individual partial wave coefficient, improving the global accuracy of the computation.

The near-trapped modes phenomenon only occurs at specific propagating directions of the incident waves, in this case for $\beta = \pi/4$, for the layout analyzed. As shown in Figure 8, the excitation force in surge for cylinders 1-2 has a sharp peak at $ka = 1.66$. Similarly to Figure 7, a very good match is observed between the results by [14] and those obtained from the application of the IT. A slight overestimation of the peaks for surge, mainly at low wave numbers ($ka < 1$), is observed for the results computed using expression (72).

Figures 9 - 12 show the variation of the radiation damping coefficients with wave number. Results are computed with the IT, making use of the hydrodynamic operators obtained with our BEM code, as well as from expression (80), and compared to [14]. In general, good agreement between the three methodologies can be observed, apart from slight under- and overestimation of the results computed using the relationship (80) at several wave numbers. Slight frequency irregularities can be detected at the same wave numbers detailed for the excitation forces. Figure 12 shows the separate contributions from the isolated body and from the hydrodynamic interaction to the diagonal radiation damping coefficients computed by means of expression (81). For the surge mode of motion, the effect of the hydrodynamic interactions is clearly observed at $ka = 1.66$.

The differences in the results by [14] obtained at low wave numbers ($ka \leq 1$) are mainly attributable to discrepancies between the semi-analytical solution and the BEM solver, which has also been shown by [20]. For the rest of the wave number range, discrepancies are due to numerical inaccuracies in the calculations performed with the methodology implemented.

5. Conclusions

Simple relationships between the Force Transfer Matrix (FTM) and the Radiation Characteristics (RC), and between the radiation damping coefficients and the FTM were obtained following two different derivations. The first identity enables faster calculation of the RC, as it removes the need to solve any radiation problem or to numerically integrate the source strengths over the wetted surface of the body, as is required by the methodology of [4].

Numerical validations of the relationships for a truncated vertical circular cylinder were carried out. Very good agreement was observed between the FTM and radiation damping coefficients computed with our BEM solver and the same quantities obtained from the RC and the FTM respectively by means of the new relationships derived.

The excitation force for a body in the array was expressed as a function of

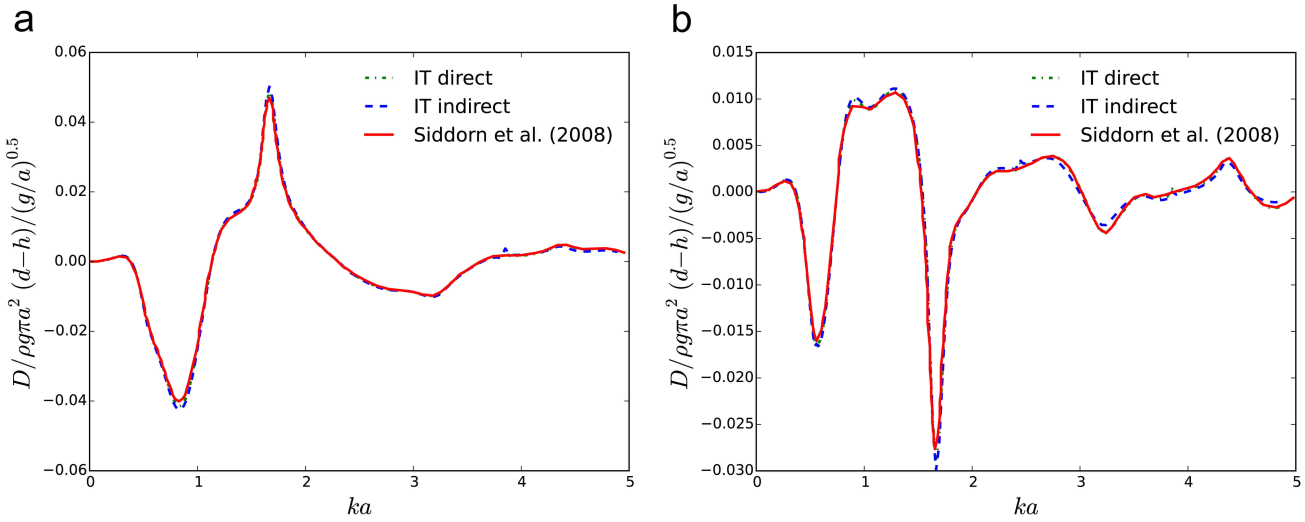

Figure 9: Non-dimensional Surge coupling radiation damping coefficients between two cylinders (1-3 in a); 1-4 in b)) in the array shown in Figure 6. The first index indicates the cylinder on which the radiation force is evaluated due to the motion of the body indicated by the second index. The solid line reproduces the results by [14]; the dotted green line has been computed with the IT by [1] using our BEM solver to compute the required hydrodynamic operators and the dotted blue line by means of the right-hand side of equation (80).

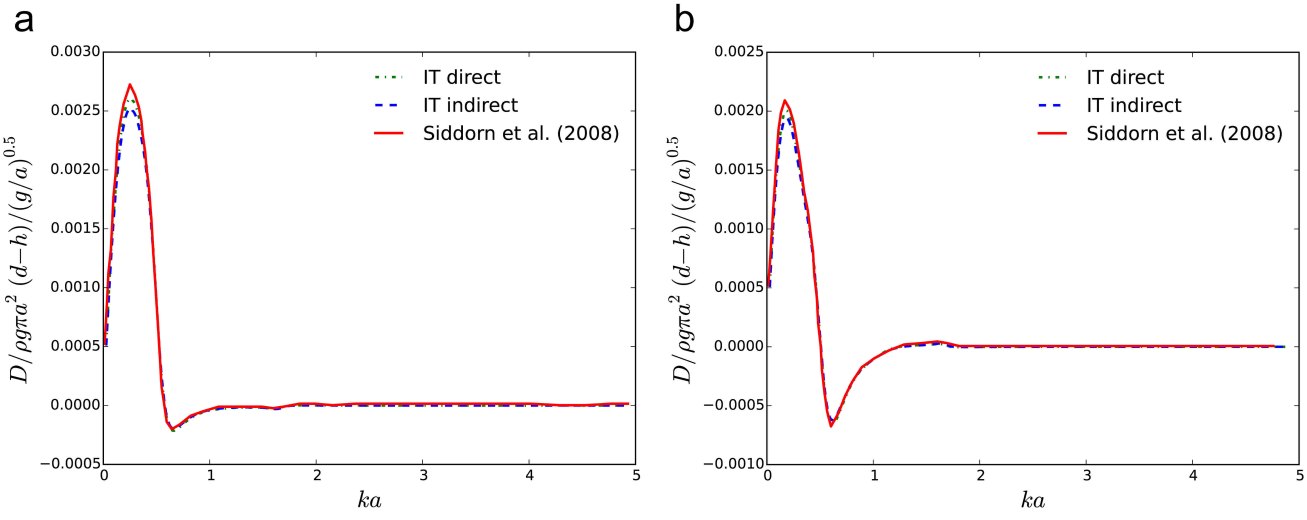

Figure 10: Non-dimensional Heave coupling radiation damping coefficients between two cylinders (1-3 in a); 1-4 in b)) in the array shown in Figure 6. The legend follows as in Figure 9.

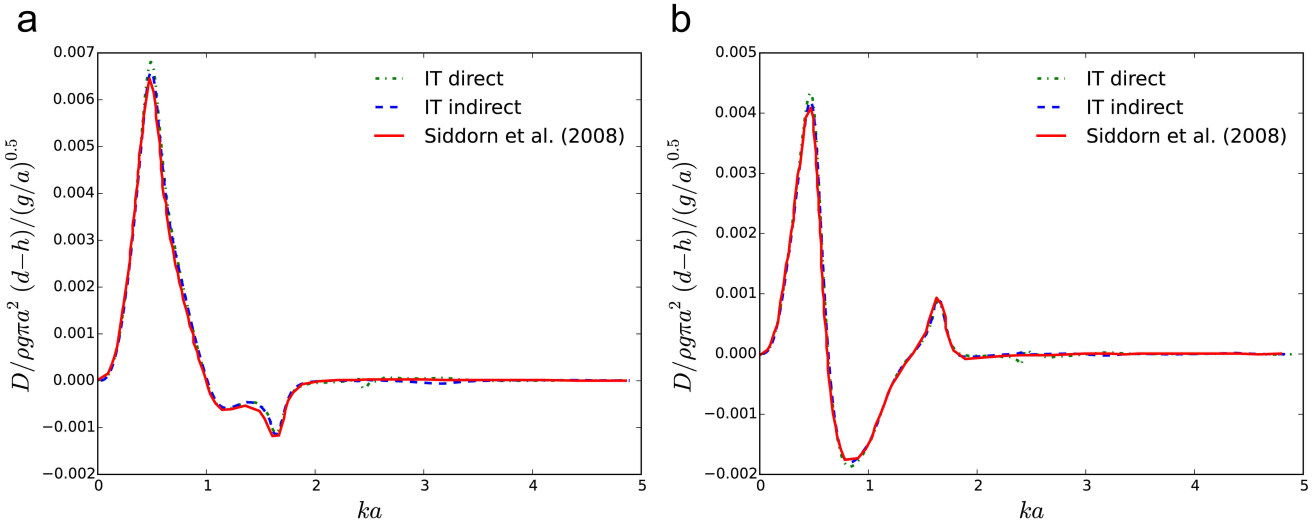

Figure 11: Non-dimensional Heave-Surge coupling radiation damping coefficients between two cylinders (1-3 in a); 1-4 in b)) in the array shown in Figure 6. The legend follows as in Figure 9.

its RC and the scattering coefficients of a radiation multiple-scattering problem. In addition, the radiation damping coefficients for the bodies in an array have been related to both their RC and the scattering coefficients of a radiation problem. Numerical verifications of these identities were performed using the array of four truncated vertical circular cylinders studied by [14]. Good agreement was obtained between their results, the standard calculation of both the excitation forces and the radiation damping coefficients using the IT with its associated hydrodynamic operators computed with NEMOH, and the same quantities calculated from both the RC and the scattering coefficients associated with a radiation problem.

The derived expressions were used to compute the separate contributions to the excitation force in surge and to the surge coupling radiation damping coefficients on a body in the array, from the body itself as if it was isolated, and from the hydrodynamic interactions with its neighbours. The effect of trapped modes at specific wavelengths, characterized by a large increase in the force on

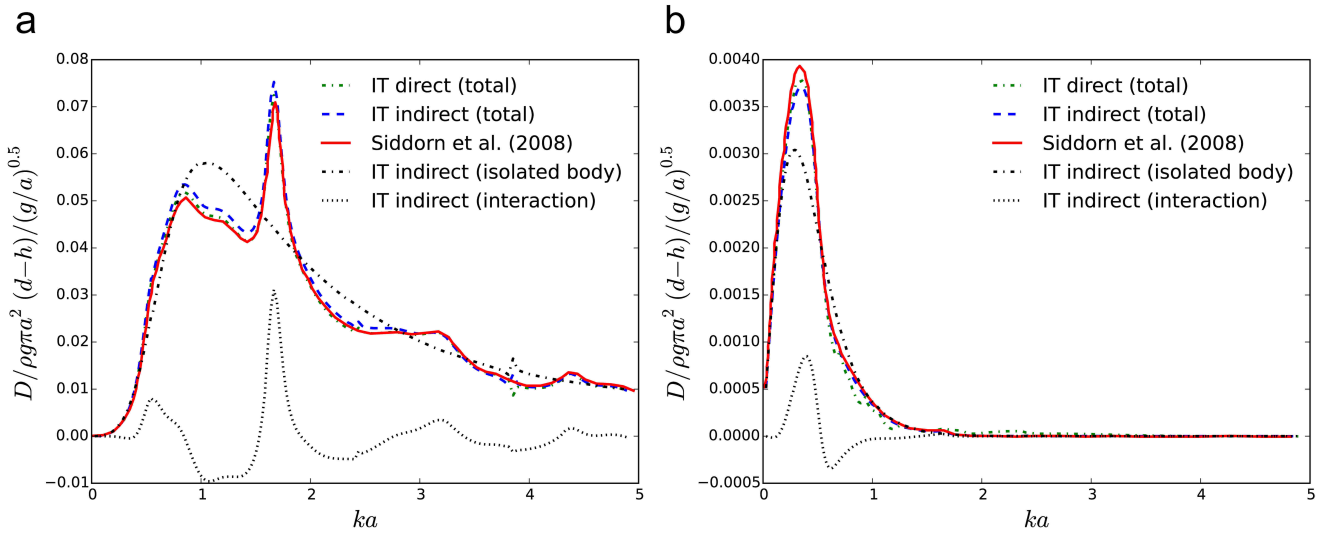

Figure 12: Non-dimensional diagonal Surge (a) and Heave (b) radiation damping coefficients of cylinder 1 in the array shown in Figure 6. The solid line reproduces the results by [14]; the dotted green line has been computed with the IT by [1] using our BEM solver to compute the required hydrodynamic operators and the dotted blue line by means of the right-hand side of equation (80). The black dotted lines $(- \cdot - \cdot)$ and $(\cdot \cdot \cdot)$ correspond respectively to the contribution to the total radiation force from the isolated body and from the hydrodynamic interactions with the neighbours and have been computed from the first and second terms of equation (81) respectively.

the body caused by hydrodynamic interactions, has been clearly observed, as expected.

It is believed that the novel relationships derived herein can be used to speed up the computation of the RC of the body, as well as to test the accuracy of the interaction theory implemented.

Acknowledgements

The research leading to these results is part of the OceaNET project, which has received funding from the European Union's Seventh Framework Programme for research, technological development and demonstration under grant agreement no 607656.

References

[1] H. Kagemoto, D. K. P. Yue, Interactions among multiple three-dimensional bodies in water waves: an exact algebraic method, Journal of Fluid Mechanics 166 (1986) 189.

[2] J. C. McNatt, V. Venugopal, D. Forehand, A novel method for deriving the diffraction transfer matrix and its application to multi-body interactions in water waves, Ocean Engineering 94 (2015) 173–185.

[3] P. A.Martin, Multiple Scattering: Interaction of Time-Harmonic Waves with N Obstacles, 2006.

[4] J.-S. Goo, K. Yoshida, A Numerical Method for Huge Semisubmersible Responses in Waves, Society of Naval Architects and Marine Engineers 98 (1990) 365–387.

[5] S. Chakrabarti, Hydrodynamic interaction forces on multi-moduled structures, Ocean Engineering 27 (2000) 1037–1063.

[6] S. Chakrabarti, Response due to moored multiple structure interaction, Marine Structures 14 (2001) 231–258.

[7] M. a. Peter, M. H. Meylan, Infinite-depth interaction theory for arbitrary floating bodies applied to wave forcing of ice floes, Journal of Fluid Mechanics 500 (2004) 145–167.

[8] M. K. U. Kashiwagi, Hydrodynamic interactions among a great number of columns supporting a very large flexible structure, Journal of Fluids and Structures 14 (2000) 1013–1034.

[9] F. Fàbregas Flavià, C. McNatt, F. Rongère, A. Babarit, A. H. Clément, A numerical tool for the frequency domain simulation of large arrays of identical floating bodies, Ocean Engineering (submitted for publication).

[10] C. C.Mei, M. Stiassnie, D. K.P.Yue, Theory and applications of ocean surface waves. Part 1: Linear Aspects, World Scientiifc Publishing, 2005.

[11] J. Falnes, Radiation impedance matrix and optimum power absorption for interacting oscillators in surface waves, Applied Ocean Research 2 (1980) 75–80.

[12] M. Haskind, The Exciting Forces and Wetting of Ships in Waves, (in Russian), Izvestia Akademii Nauk S.S.S.R., Otdelenie Tekhnicheskikh Nauk, No. 7 (English translation available as David Taylor Model Basin Translation No. 307, March 1962), 1957.

[13] J. C. McNatt, V. Venugopal, D. Forehand, The cylindrical wave field of wave energy converters, International Journal of Marine Energy 3-4 (2013) e26–e39.

[14] P. Siddorn, R. Eatock Taylor, Diffraction and independent radiation by an array of floating cylinders, Ocean Engineering 35 (2008) 1289–1303.

[15] J. Newman, The Exciting Forces on Fixed Bodies in Waves, Journal of Ship Research 6 (1962).

[16] G. Watson, A treatise on the theory of Bessel functions, Cambridge University Press, 1966.

[17] M. Abramowitz, I. Segun A., Handbook of mathematical functions with Formulas, Graphs, and Mathematical Tables, first ed., Dover Publications, Inc, 1964.

[18] J. Falnes, Ocean Waves and Oscillating Systems, Cambridge University Press, 2002.

[19] J. N. Newman, Marine Hydrodynamics, 9th ed., The Massachusetts Institute of Technology, 1977.

[20] J. Cruz, R. Sykes, P. Siddorn, R. Taylor, Estimating the loads and energy yield of arrays of wave energy converters under realistic seas, IET Renewable Power Generation 4 (2010) 488–497.